

## Thermodynamic Characterization of the Conformational Stability of the Homodimeric Protein, Pea Lectin<sup>†</sup>

Nisar Ahmad, V. R. Srinivas, G. Bhanuprakash Reddy, and Avadhesh Surolia\*

*Molecular Biophysics Unit, Indian Institute of Science, Bangalore-560012, India*

*Received May 18, 1998; Revised Manuscript Received September 11, 1998*

**ABSTRACT:** The conformational stability of the homodimeric pea lectin was determined by both isothermal urea-induced and thermal denaturation in the absence and presence of urea. The denaturation profiles were analyzed to obtain the thermodynamic parameters associated with the unfolding of the protein. The data not only conform to the simple  $A_2 \rightleftharpoons 2U$  model of unfolding but also are well described by the linear extrapolation model for the nature of denaturant–protein interactions. In addition, both the conformational stability ( $\Delta G_s$ ) and the  $\Delta C_p$  for the protein unfolding is quite high, at about 18.79 kcal/mol and 5.32 kcal/(mol K), respectively, which may be a reflection of the relatively larger size of the dimeric molecule ( $M_r$  49 000) and, perhaps, a consequent larger buried hydrophobic core in the folded protein. The simple two-state ( $A_2 \rightleftharpoons 2U$ ) nature of the unfolding process, with the absence of any monomeric intermediate, suggests that the quaternary interactions alone may contribute significantly to the conformational stability of the oligomer—a point that may be general to many oligomeric proteins.

Equilibrium denaturation and kinetic studies on the folding/unfolding of proteins have largely been done on small monomeric globular proteins. The high degree of reversibility, unimolecular folding kinetics, less complexity in handling, and the feasibility of NMR structure solution have made the small, monomeric globular proteins attractive as systems for these studies (1–6). Though these studies have provided much information on the forces and energetics involved in the folding and packing of proteins (7, 8), similar studies on oligomeric proteins have been less common and the information regarding their folding has been relatively less (9–12, 38–41). Though the folding of individual polypeptide chains of multimeric proteins might be similar to that of single-chain proteins, they would, in addition, be accompanied by simultaneous interactions with the other monomers. Thus the folding pathway would involve both intramolecular and intermolecular interactions. Moreover, by their very nature, the role of subunit–subunit interactions in the overall stability and integrity of proteins can be addressed only in oligomeric proteins.

Legume lectins, a family of proteins that bind carbohydrates specifically and reversibly, have very highly similar tertiary structure, but widely different quaternary associations (13). The tertiary structure of each monomeric unit of legume lectins consists of two antiparallel  $\beta$ -pleated sheets, of which the plane of one is flat and the other twisted by 90° along an axis perpendicular to the chain segments. For

some of the lectins, such as ECorL, WBA I, and GS4, the differences in quaternary association, which affect the association and reduce the extent of the intersubunit interface thereby rendering them less stable, have been attributed to the presence of glycosylation (14–15). This is in contrast to pea, con A, and lentil lectin (all nonglycosylated proteins), where the monomers can come together in such a way that the two  $\beta$  sheets interact through hydrophobic interactions and hydrogen bonds and form a 12-stranded contiguous sheet, described as the typical “canonical dimer”. The subunit interface in these lectins is much more extensive (1000 Å), as compared to ECorL (700 Å), GS4, and WBA I, rendering them more stable (16). Thus legume lectins can be described as “natural mutants of quaternary structures” and hence can, in general, serve as interesting model systems for the study of the influence of glycosylation and intersubunit interface on the folding of oligomeric proteins. In the present investigation we have carried out a rigorous thermodynamic study, the first for an oligomeric legume lectin member, on the stability of the pea lectin by solution denaturation, using fluorescence and circular dichroism as probes for the process of unfolding. The pea lectin (a nonglycosylated lectin) exists as a dimer, has a  $M_r$  49 000, requires  $Ca^{2+}$  and  $Mg^{2+}$  ions for carbohydrate binding, and has a single carbohydrate binding site per monomer (17). Each of the pea lectin monomers consists of an  $\alpha$  and a  $\beta$  chain. The crystal structure of pea lectin shows that the polypeptide chain takes a convoluted pathway to form 2 major and 1 minor antiparallel  $\beta$  sheet structures (17). Extensive random coil structures are overlaid onto the front of the molecule. The two monomers join together to form the typical canonical dimer. In this paper we show that the unfolding of pea lectin can be described as a two-state process, where the unfolding and dissociation are closely related and can be described in terms of an equilibrium

<sup>†</sup> This work has been supported by grants from the Department of Science and Technology, Government of India, Council of Scientific and Industrial Research, India. N.A. is a Research Associate supported by the Department of Science and Technology, Government of India and G.B.R. is part of the Postdoctoral Fellow program of the Department of Biotechnology, Government of India.

\* Corresponding author: Molecular Biophysics Unit, Indian Institute of Science, Bangalore-560012, India. Fax: 91-80-3348535/3341683. Tel: 91-80-3092389. E-mail: suroli@mbu.iisc.ernet.in.

population of folded dimers and unfolded monomers, and obtain estimates of its conformational stabilities. The data, in addition, were consistent with the linear extrapolation model for protein–urea interactions.

## MATERIALS AND METHODS

**Materials.** 3,3'-Dimethyl glutaric acid (DMG) and extrapure urea were purchased from Sigma Chemical Co. All other reagents used for this study were of the highest purity available. Stock urea solutions were prepared fresh in 50 mM sodium phosphate buffer, pH 7.2, and the molarity of urea was determined by refractive index as described by Pace (20).

**Protein Purification.** Pea lectin was purified from pea seeds by affinity chromatography (18). The purity was checked by SDS–PAGE. The concentration of the protein solution was determined from its specific extinction coefficient  $A_{280}^{1\%} = 15$  (19).

**Isothermal Urea-Induced Denaturation.** Equilibrium unfolding as a function of urea concentration was monitored by fluorescence spectroscopy, near- and far-UV CD. The fluorescence measurements were done on a JASCO FP777 spectrofluorimeter in a 1 cm water-jacketed cell. The excitation and emission wavelengths were fixed at 282 and 319 nm, respectively, with slit widths of 5 nm for both monochromators. Each measurement was an average of four readings. The CD measurements were made on a JASCO-J-500A spectropolarimeter attached to a DP-501N data processor. Far-UV CD was followed at 222 nm in a 0.1 cm path length cell and the near-UV CD monitored at 270 nm in a 0.5 cm path length cell. The spectra were collected with a slit width of 1 nm, a response time of 8 s, and a scan speed of 10 nm s<sup>-1</sup>. Each data point was an average of 8 accumulations for far-UV CD and 4 accumulations for near-UV CD. Protein concentrations of 4, 8, and 20  $\mu$ M were used. Reversibility was checked by fluorescence and near- and far-UV CD by the return of the complete spectrum upon unfolding with 9.5 M urea followed by dilution to a final protein concentration of 8  $\mu$ M and a urea concentration of 0.5 M.

Twelve isothermal urea-induced denaturation curves were collected in the range of temperature between 277 and 328 K. The temperature of the cuvette was monitored using a digital temperature probe. A Julabo water bath was used for maintaining the sample temperature to within  $\pm 0.1$  K of the set temperature.

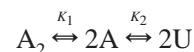
**Thermal Denaturation Transitions.** Thermal denaturation transitions were carried out in the presence and absence of urea on JASCO-J-500A spectropolarimeter attached to a DP-501N data processor by following the far-UV spectrum. Data were collected after 12 h of incubation of the samples. The reversibility of thermal scans was monitored by the return of the CD spectrum after cooling from 85 to 20° C.

**Differential Scanning Calorimetry.** DSC measurements at different pH's were performed with a Microcal MC-2 DSC heat conduction scanning calorimeter which consists of two fixed 1.2 mL cells, a reference cell, and a solution cell. The measurements were usually at a scan rate of 20 K h<sup>-1</sup>. The

protein solutions were prepared in the appropriate buffer by diluting a stock protein solution to get the final concentration of 0.3 mM, dialyzed for 6 h in a large volume of the same buffer and centrifuged to remove any insoluble material. Three different buffers, acetate, DMG, and phosphate, were used in their appropriate pH range, namely, 4.3–5.8 for acetate, 6.2–6.8 for DMG, and 7.2 for phosphate. The data obtained at all the pH's were analyzed using the ORIGIN DSC program provided by Microcal Inc. assuming the two-state process  $N_2 \rightleftharpoons 2U$ .

## RESULTS

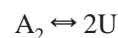
The analysis of denaturation curves is based on the assumption that only two states, the native and the denatured forms, exist at equilibrium. Such an assumption may not apply for dimeric (or oligomeric) proteins because intrachain and interchain interactions would make distinct contributions to the overall protein conformational stability. Completely unfolded dimers are unlikely to exist, whereas there is a provision for the native-like compact monomeric state. Thus the overall unfolding reaction may start with the folded dimer ( $A_2$ ) and end with two unfolded monomers (11). Hence, if both the folded monomer and folded dimer are significantly populated in the transition region, a three-state model comprising equilibrium dissociation of dimer into monomers followed by their unfolding to random coils may have to be applied for the transitions of these proteins. Thus the overall reaction maybe described by the following:



where  $K_1 = [A]^2/[A_2]$  and  $K_2 = [U]/[A]$ .

For such a kind of transition one might see biphasic denaturation curves or non-superimposable transitions when different spectroscopic probes are used to follow the change. As can be seen in Figure 1 the urea denaturation scan profiles, when monitored by fluorescence, far-UV CD, and near-UV CD, are completely superimposable which is thus evidence against the non-two-state possibility. Therefore one can expect either a direct  $A_2 \rightleftharpoons 2U$  transition, where the folded monomer is insignificantly populated, or a  $2A \rightleftharpoons 2U$  kind of transition in which there is a rapid dissociation of the dimer followed by an equilibrium between the folded and unfolded monomers.

In the former case the above equation may be simplified to include only folded dimers and unfolded monomers:



where  $K_u = [A]^2/[U]$ . In this case the stability of the protein would increase with higher concentration and the dimeric state must be significantly populated in the transition zone. Hence the equilibrium constant would be given by the following:

$$K_u = 2P_t f_u^2 / (1 - f_u)$$

where  $P_t$  is the total monomeric protein concentration and  $f_u$  is the molar fraction of the unfolded protein as monitored by a specific spectroscopic probe. If, on the other hand, the dimer dissociates prior to the transition zone of the denaturation profiles, then, only equilibrium between folded

<sup>1</sup> Abbreviations: DMG, 3,3-dimethylglutarate; LEM, linear extrapolation model.

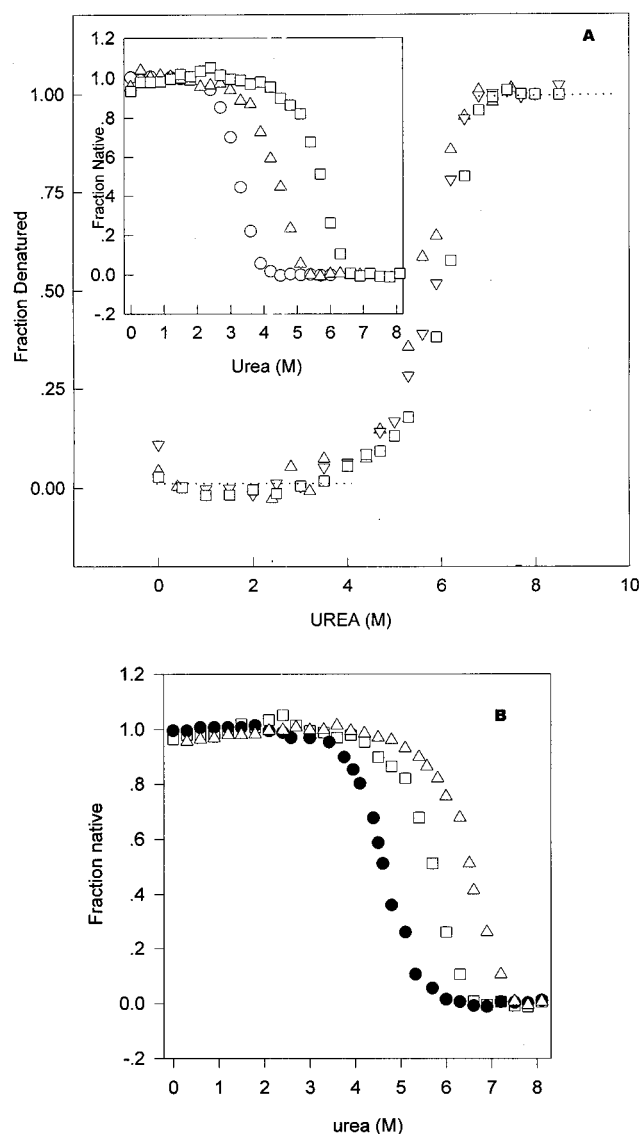
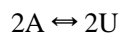


FIGURE 1: (A) Urea-induced denaturation curves monitored by fluorescence (O) and near-UV CD (Δ) at 298 K. The concentration of protein used was 8 μM in 50 mM phosphate buffer (pH 7.2). The dotted straight lines in the figure are the pre- and post-transition regions of the curve. (Inset) Urea-induced denaturation curves at three different temperatures monitored by fluorescence: 277 K (O), 298 K (□), and 313 K (Δ). (B) Concentration of pea lectin dependence on urea denaturations monitored by fluorescence: (●) is pea lectin concentration at 4 μM, (□) at 8 μM, and (Δ) at 20 μM. The  $\Delta G_{H_2O}$  = 18.31, 18.47, and 18.49 kcal/mol at protein concentrations 4, 8, and 20 μM, respectively.

monomers and unfolded monomers would be observed:



$$K_u = [U]/[A]$$

Such a reaction would be unimolecular, and the equilibrium populations of the folded and unfolded protein would be independent of the protein concentration.

In our case we observe that there is a distinct dependence of the unfolding profiles on protein concentration (Figure 1B) such that we obtain the same values for  $K_u$  (and  $\Delta G_u$ ). Also on gel filtration, on a Biogel P100 column, the protein (8 μM concentration) elutes as a dimer in the region of urea concentration (0–4 M urea) where only the folded form is

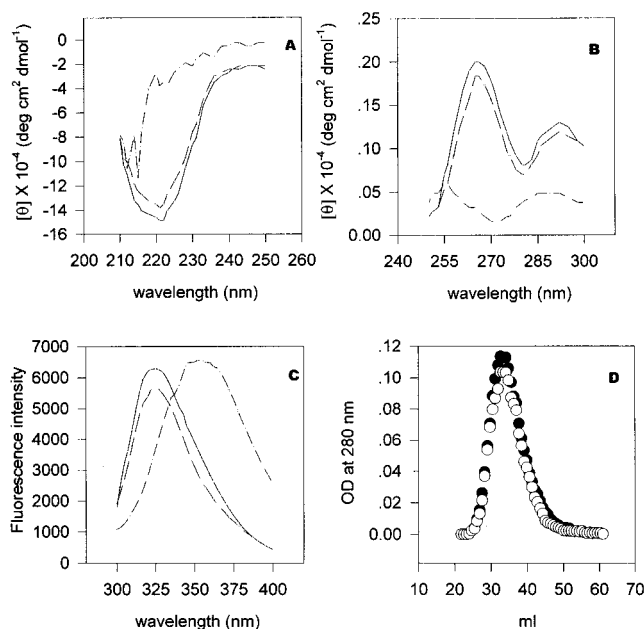


FIGURE 2: (A–C) Native and refolded spectrum of pea lectin as monitored by (A) far-UV CD, (B) near-UV CD, and (C) fluorescence spectrum. The respective values were plotted for every 2–3 nm. The spectrum of the refolded protein obtained after thermal denaturation was monitored by far- and near-UV CD. There is a complete overlap between the spectrum of both kinds of refolded protein; hence only a single spectrum is shown: continuous line (—), spectrum of the native protein; discontinuous line (---) spectrum of the refolded protein; serrated line (— · — ·), spectrum of denatured protein. (D) Gel filtration profile of the native (●) and refolded protein (○) on a Biogel P 100 column (length, 90 cm; diameter, 1 cm). The elution volume of blue dextran is 23 mL.

seen, while in the region (above 6.8 M) where only the denatured species is noted, only the unfolded monomers are seen. In the transition region (4–6.0 M) the amounts of folded dimers and unfolded monomers are proportional to those expected from the spectroscopic studies. The unfolding of the pea lectin results in its demetallization, yet the unfolding is almost completely reversible, after urea and thermal denaturation, (85%–90%) as monitored spectroscopically (Figure 2 A–C). In addition, reversibility at the quaternary structural level of the protein was confirmed by gel filtration, on a Biogel P100 column. The refolded protein eluted as a single peak and at the same position as that of the native protein (Figure 2C). In view of the almost complete reversibility and the observation of a good correlation between the data obtained from thermal and chemical denaturation, the transitions are treated as the two-state  $A_2 \rightleftharpoons 2U$  process. This, in addition, corroborates our earlier DSC studies where we have proposed that the lectin undergoes a two-state  $A_2 \rightleftharpoons 2U$  transition (16).

**Data Analysis.** The denaturation of proteins is usually accompanied by a large change in the heat capacity ( $\Delta C_p$ ). This parameter is used as a measure of the hydrophobicity of the protein and provides a direct relationship to other thermodynamic quantities,  $\Delta H$ ,  $\Delta S$ , and  $\Delta G$ , from eqs 1, 2, and 3, respectively (21, 22).

$$\Delta H(T) = \Delta H_g + \Delta C_p(T - T_g) \quad (1)$$

$$\Delta S(T) = \Delta S_g + \Delta C_p \ln(T/T_p) \quad (2)$$

$$\Delta G = \Delta H - T\Delta S \quad (3)$$

Thus,

$$\Delta G(T) = \Delta H_g(1 - T/T_g) + \Delta C_p[(T - T_g) - T \ln(T/T_g)] \quad (4)$$

where  $T_g$  is the temperature where  $\Delta G = 0$ .

According to the linear free-energy model (LEM) (22, 23), the changes in the Gibbs free energy, enthalpy, entropy, and heat capacity that accompany protein unfolding have a linear dependence on the molar concentration of the denaturant, namely,

$$\Delta G_u = \Delta G_{(H_2O)} + m[\text{urea}] \quad (5)$$

$$\Delta S_u = \Delta S_{(H_2O)} + s[\text{urea}] \quad (6)$$

$$\Delta H_u = \Delta H_{(H_2O)} + h[\text{urea}] \quad (7)$$

$$\Delta C_{up} = \Delta C_{p(H_2O)} + c[\text{urea}] \quad (8)$$

$\Delta G_u$ ,  $\Delta S_u$ ,  $\Delta H_u$ , and  $\Delta C_{up}$  represent the respective parameters obtained in the presence of a known urea concentration.

**Isothermal Urea Denaturation Curves.** The urea denaturation curves were analyzed to obtain  $\Delta G_{(H_2O)}$ , the free energy of unfolding in water at any temperature as follows.

The  $\Delta G_u$ , the free energy of unfolding at various urea concentrations for each of the isothermal urea denaturation profiles, can be calculated from eqs 9a and 9b (11).

$$\Delta G_u = -RT \ln K_u \quad (9a)$$

where

$$K_u = 2P_t[f_u^2/(1 - f_u)] \quad (9b)$$

The  $\Delta G_{(H_2O)}$  can now be calculated from eq 5. Typical unfolding profiles as monitored by urea-induced denaturation are shown in Figure 1A. The straight lines in the Figure 1A indicate the pre- and post-transition regions of the curves. Twelve isothermal urea-induced denaturation curves were obtained in the temperature range from 277 to 328 K. The inset in Figure 1 shows the urea-induced denaturation at 3 different temperatures. Also shown in Figure 1B is the fluorescence urea denaturation profiles at 3 different protein concentrations (4, 8, 20  $\mu$ M) at 298 K. With increasing protein concentration, the fraction of the native molecules increases. Similar protein concentration dependence was observed when monitored by both near- and far-UV CD and for thermal denaturation (as monitored by far-UV CD). Equations 9 (a and b) and 5 were used to obtain the values of  $\Delta G_{(H_2O)}$ . These values are shown in Table 1. The plots of  $\Delta G_{(H_2O)}$ ,  $m$ , and  $C_m$  versus temperature are shown in Figure 3 A–C. Here the  $C_m$  is defined by the equation  $\{RT \ln [\text{protein}] + \Delta G_{(H_2O)}\}/m$  (11). It can be clearly seen that the protein becomes less stable (Figure 3A,B) at temperatures above and below 300 K. The value of  $m$ , defined as the gradient of change in the folding free energy with molar concentration, seems to be independent of temperature (Figure 3C).

**Thermally Induced Denaturation Curves.** The thermal transitions in the absence and presence of urea were first

Table 1: Analysis of the Urea Denaturation Curves at Different Temperatures<sup>a</sup>

| temperature<br>(K) | $C_m$<br>(M urea) | $\Delta G_{(H_2O)}$<br>(kcal/mol) | $m$<br>(kcal/(mol M)) |
|--------------------|-------------------|-----------------------------------|-----------------------|
| 277                | 4.59              | 14.02                             | −2.90                 |
| 283                | 5.72              | 15.57                             | −2.59                 |
| 288                | 6.47              | 17.52                             | −2.59                 |
| 293                | 6.91              | 18.32                             | −2.63                 |
| 298                | 6.79              | 18.48                             | −2.61                 |
| 301                | 7.44              | 18.53                             | −2.39                 |
| 303                | 6.79              | 18.21                             | −2.35                 |
| 310                | 6.34              | 17.95                             | −2.70                 |
| 313                | 6.65              | 17.48                             | −2.51                 |
| 318                | 6.54              | 16.82                             | −2.45                 |
| 323                | 4.12              | 14.17                             | −3.24                 |
| 328                | 5.66              | 12.47                             | −2.05                 |

<sup>a</sup> The  $C_m$  is defined by the equation  $\{RT \ln [\text{protein}] + \Delta G_{(H_2O)}\}/m$ . The urea denaturation profiles were analyzed assuming the linear extrapolation model, using eq 5 to obtain  $\Delta G_{(H_2O)}$ .

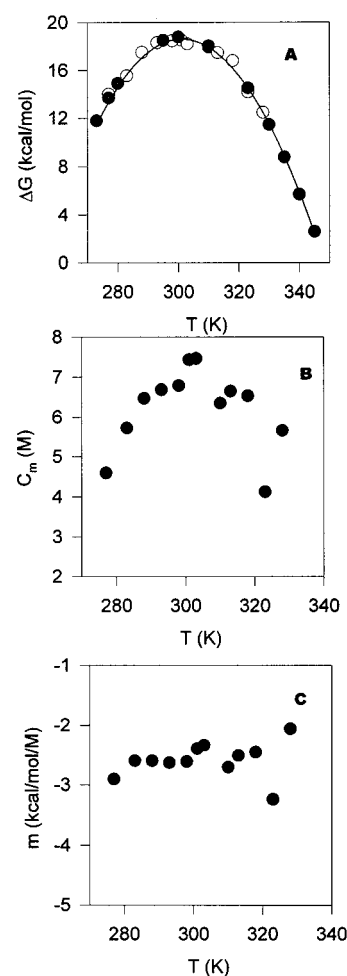


FIGURE 3: Unfolding free energy,  $C_m$ , and  $m$  as a function of temperature. (A) Unfolding free energy as a function of temperature. The open circles, (O), are  $\Delta G_{(H_2O)}$  values obtained from urea denaturations at various temperatures using eq 5. The closed circles (●) represent unfolding free energies obtained from thermal denaturation in the absence of urea. The continuous line shows the least-squares fit of the points to eq 4. The standard error of the fits for the  $\Delta C_p$  parameter was 0.8%. (B)  $C_m$  as a function of temperature for the urea denaturation curves in the temperature range 277–328 K. (C)  $m$  (obtained from fitting the urea denaturation profiles to eq 5) as a function of temperature.

converted to fraction denatured ( $f_u$ ) and fraction native ( $f_n$ ) terms. The apparent free-energy change at any temperature



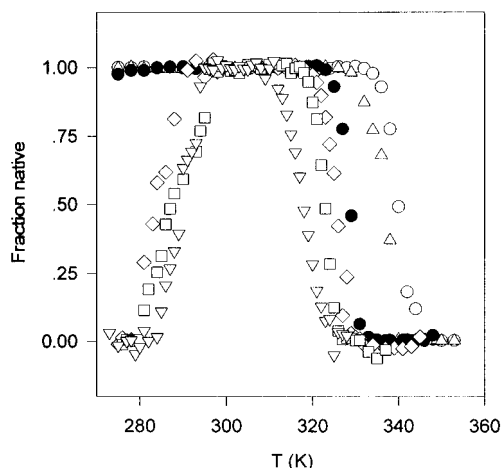


FIGURE 4: Thermal denaturation of pea lectin, monitored by far-UV CD. Thermal scans in the absence (○) and presence of 1 M (●), 3.8 M (◇), 5.5 M (□), 5.7 M (□), and 6 M (▽) urea.

of the transition is obtained by the following equation:

$$\Delta G = -RT \ln K_{\text{app}} \quad (10)$$

where

$$K_{\text{app}} = 2P_{\text{f}}^2 / (1 - f_{\text{u}}) \quad (11)$$

Thermal unfolding curves obtained, using far-UV CD, in the absence and presence of urea are shown in Figure 4. The heat denaturation is shifted to lower temperatures with an increase in urea concentration. Cold denaturation can be clearly seen beyond 3.8 M urea. The cold denaturations were observed to be completely reversible. At concentrations higher than 6.5 M urea, the protein was completely unfolded and no transitions were seen. For the thermal transitions, the apparent free-energy change at any temperature (in the absence and presence of urea) may be obtained (as mentioned above) from eqs 10 and 11. The data so obtained may then be fitted to eq 4 to provide estimates of  $\Delta H_{\text{g}}$ ,  $\Delta S_{\text{g}}$ , and  $\Delta C_{\text{p}}$  at each urea concentration, where  $\Delta H_{\text{g}}$  and  $\Delta S_{\text{g}}$  are the enthalpies and entropies at  $T_{\text{g}}$ , the temperature at which  $\Delta G = 0$ . These results are presented in Table 2 A,B. The thermodynamic parameters for cold denaturation were also determined using the same stability curves, with the constraint that  $\Delta H_{\text{g}} < 0$ . All of the thermodynamic parameters thus obtained are shown in Table 2 A,B. The  $\Delta C_{\text{p}}$  values, as expected, were nearly the same, within experimental error, for both cold- and high-temperature transitions. The temperature of maximum stability ( $T_{\text{s}}$ ), ( $T_{\text{h}}$ ), the temperature at which the enthalpy is zero and the conformational stability at  $T_{\text{s}}$  ( $\Delta G_{\text{s}}$ ) can be obtained for each of the curves by the following equations (25):

$$\ln(T_{\text{g}}/T_{\text{s}}) = \Delta H_{\text{g}}/T_{\text{g}}\Delta C_{\text{p}} \quad (12)$$

$$T_{\text{h}} = T_{\text{g}} - \Delta H_{\text{g}}/\Delta C_{\text{p}} \quad (13)$$

$$\Delta G_{\text{s}} = \Delta C_{\text{p}}(T_{\text{s}} - T_{\text{h}}) \quad (14)$$

**Evaluation of Thermodynamic Parameters of Pea Lectin—Urea Interactions.** The free-energy values obtained from thermal denaturations in the absence and presence of urea (as described in the previous section) can be used to evaluate

urea dependence of the thermodynamic parameters as a test of the linear extrapolation model. The  $\Delta H_{\text{(T)}}$ ,  $\Delta S_{\text{(T)}}$ ,  $\Delta G_{\text{(T)}}$ , and  $\Delta C_{\text{p}}$  can be evaluated at any temperature using eqs 1–3. These values were calculated for several temperatures between 275 and 350 K to prove the linear relationship between thermodynamic parameters and molar concentrations of urea. The values obtained at 277, 295, and 310 K have been shown in Figure 5 A–C. The values of  $\Delta H_{\text{(T)}}$  and  $\Delta S_{\text{(T)}}$  at each temperature vary such that the resultant value of  $\Delta G_{\text{(T)}}$  decreases linearly with urea concentration, as enunciated in the linear free-energy model. The calculated values of  $\Delta G_{\text{(T)}}$  for the thermal denaturation of the native protein (in the absence of urea) are plotted against various temperatures in Figure 3A, along with  $\Delta G_{\text{H}_2\text{O}}$  calculated from isothermal urea-induced denaturations at their respective temperatures. The open circles (○) are the  $\Delta G_{\text{H}_2\text{O}}$  values obtained from the urea denaturation profile, using eq 5, and the closed circles (●) are the calculated  $\Delta G_{\text{(T)}}$  values obtained from the thermal denaturation of the protein in the absence of urea, using eq 1–3. The coincidence of the two data sets provides further confirmation of the applicability of the linear free-energy model. Similar coincidences were also observed for values of  $\Delta G_{\text{(T)}}$  as a function of temperature for thermal denaturations in the presence of urea (data not shown).

## DISCUSSION

Legume lectins exist as oligomers. Earlier differential scanning calorimetric studies in our laboratory have shown that most of them undergo simultaneous dissociation upon unfolding. What was not clear was whether dissociation precedes unfolding or vice versa. Therefore, a more extensive study of urea-induced denaturation of the pea lectin at various temperatures and also as a function of temperature in the presence and absence of denaturant was carried out. This allows us to understand the process of dissociation in relation to the unfolding of the pea lectin and to calculate the stability of the protein in terms of its free energy of unfolding. The principal observations of this study are the following: (1) The unfolding of pea lectin is a simple two state process, namely,  $A_2 \rightleftharpoons 2U$ ; (2) It undergoes cold denaturation, which becomes distinct in thermal denaturation profiles above 3.8 M urea concentration; (3) The data are consistent with the temperature independence of  $\Delta C_{\text{p}}$  over a wide temperature range; (4) The analysis of the stability curves supports the use of the linear extrapolation model for the thermodynamic stability of pea lectin.

The urea-induced and thermal denaturation of pea lectin have been followed by fluorescence and far-UV CD, respectively. The analysis of these curves was made by assuming the unfolding reaction to be a simple two-state transition. The unfolding curves obtained by different spectroscopic probes were superimposable, but showed distinct concentration dependence and in addition were spectroscopically reversible. Moreover, upon unfolding (from thermal and urea-induced denaturation) followed by refolding, the refolded protein elutes at the same position as the native upon gel filtration Figure 2A–C. The unfolding of the pea lectin results in its demetallization. But demetallization, perhaps, results in a very local perturbation of the short region where the metal ions are expected to coordinate. This region is perhaps so small as to be insignificant in its

Table 2

| Thermodynamic Parameters for the Thermal Unfolding of Pea Lectin <sup>a</sup> |           |                         |                             |                             |           |           |                         |
|---|-----------|-------------------------|-----------------------------|-----------------------------|-----------|-----------|-------------------------|
| urea (M)  | $T_g$ (K) | $\Delta H_g$ (kcal/mol) | $\Delta S_g$ (kcal/(mol K)) | $\Delta C_p$ (kcal/(mol K)) | $T_s$ (K) | $T_h$ (K) | $\Delta G_s$ (kcal/mol) |
| 0.0   | 348.0     | 270.3                   | 0.78                        | 5.32                        | 300.72    | 297.18    | 18.83                   |
| 1.0   | 343.5     | 265.3                   | 0.77                        | 5.72                        | 300.0     | 297.09    | 17.17                   |
| 3.8   | 339.8     | 254.6                   | 0.75                        | 6.23                        | 301.29    | 298.92    | 14.77                   |
| 5.5   | 337.3     | 245.8                   | 0.73                        | 6.32                        | 300.57    | 298.41    | 13.66                   |
| 5.7   | 336.1     | 243.3                   | 0.72                        | 6.41                        | 300.22    | 298.15    | 13.23                   |
| 6.0   | 334.2     | 239.1                   | 0.71                        | 6.55                        | 299.63    | 297.71    | 12.57                   |

| Cold Denaturation Parameters <sup>b</sup> |              |                            |
|---|--------------|----------------------------|
| urea (M)                                  | $T_{gc}$ (K) | $\Delta H_{gc}$ (kcal/mol) |
| 0.0                                       | 255.5        | -268.32                    |
| 1.1                                       | 260.1        | -263.3                     |
| 3.8                                       | 266.0        | -254.12                    |
| 5.5                                       | 270.06       | -245.62                    |
| 5.7                                       | 271.01       | -242.5                     |
| 6.0                                       | 273.0        | -238.01                    |

<sup>a</sup>  $\Delta H_g$ ,  $\Delta S_g$ ,  $\Delta C_p$ , and  $T_g$  were by calculated from the thermal denaturation profiles (Figure 4) as described in the text.  $T_s$ ,  $T_h$ , and  $\Delta G_s$  were obtained from eqs 12–14. <sup>b</sup>  $T_{gc}$  and  $\Delta H_{gc}$  were obtained from thermal denaturation profiles (Figure 4A–D), by fitting the data to eq 4 with the constraint  $\Delta H_{gc} < 0$ . The  $\Delta C_p$  obtained was thus the same, within experimental error, as the values obtained for heat denaturation.

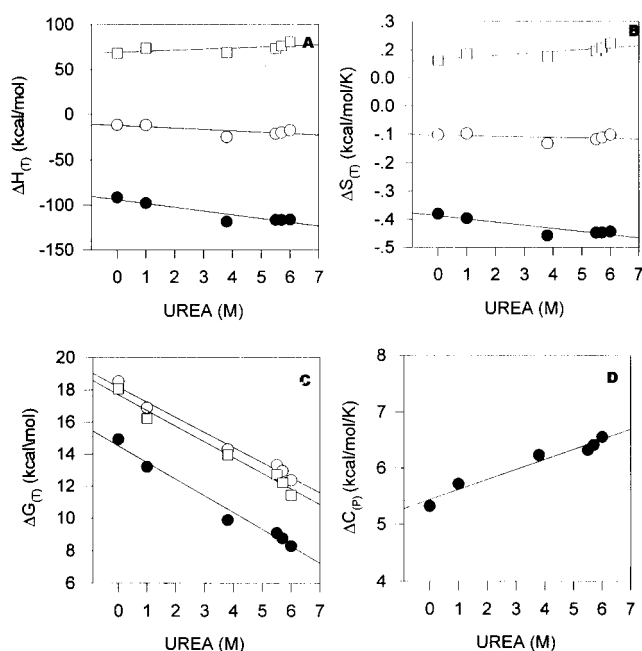


FIGURE 5: Urea dependence of various thermodynamic factors. (A) Urea dependence of  $\Delta H_{(T)}$  at 277 (●), 295 (○), and 310 K (□). (B) Urea dependence of  $\Delta S_{(T)}$  at 277 (●), 295 (○), and 310 K (□). (C) Urea dependence of  $\Delta G_{(T)}$  at 277 (●), 295 (○), and 310 K (□). (D) Urea dependence of  $\Delta C_p$ . The thermodynamic parameters in the figures were obtained from the thermal denaturation profiles (Figure 4 A–D), using eqs 1–5.

contribution to the protein conformation. Consequently the unfolding transition may be treated as a two-state  $A_2 \rightleftharpoons 2U$ .

The isothermal urea denaturation curves in the inset of Figure 1 and the stability curve, Figure 3A, both clearly show that the pea lectin undergoes cold denaturation, the temperature of maximum stability being 300 K. Cold denaturation is also distinct in the thermal denaturation scans at urea concentrations above 3.8 M (Figure 3). Some of the criteria for cold denaturation of the proteins (24, 25) include, for one, the temperature of maximum stability must be well above 273 K. For pea lectin it is 300 K. Though the maximum conformational stability,  $\Delta G_s$ , for the pea lectin is quite high, at 18.79 kcal/mol, it still conforms to the next

but important criterion, that is, a low value for the ratio of  $\Delta H/\Delta C_p$ . For pea lectin the  $\Delta H$  at 300 K is 14.96 kcal/mol, but the  $\Delta C_p$  (obtained by fitting the stability curves (Figure 3A) to eq 4) is quite high at 5.32 kcal/(mol K). Hence  $\Delta H/\Delta C_p$  is very low. Thus, the pea lectin conforms to this final criterion for observable cold denaturation. For another protein, the maltose-binding protein, a large protein of 370 amino acids, we have estimated the value of  $\Delta C_p$  to be 7.9 kcal/(mol K). This is much higher than for most globular proteins, and we have shown that the temperature at which the protein undergoes cold denaturation depends primarily on  $\Delta C_p$  and may perhaps increase with an increase in  $\Delta C_p$  (26, 27).

We have used a combination of urea and thermal denaturation experiments to investigate the thermodynamics of denaturant–pea lectin interaction and to test the validity of the linear extrapolation model (LEM) for the protein denaturation. LEM is the widely used model for the determination of the conformational stability of proteins (29) and has been rationalized by Schellman and his colleagues (30, 31). A second model proposed by Tanford (32), called a denaturant binding model, has been recently used to find out the thermodynamics of protein denaturant interactions. The difference between the two models is the selected dependence on denaturant concentrations. The binding model predicts a logarithmic dependence whereas the linear extrapolation model assumes a linear dependence of denaturant concentrations of conformational stability. As can be seen in Figure 5 our data seem to be consistent with the linear extrapolation model (LEM). From the thermal denaturation profiles (Figure 4), for all concentrations of urea, the  $\Delta H_{(T)}$ ,  $\Delta S_{(T)}$ , and  $\Delta G_{(T)}$  can be evaluated at various temperatures using eqs 1–3 in conjunction with  $\Delta H_g$ ,  $\Delta S_g$ , and  $T_g$  and  $\Delta C_p$ . In Figure 4, the  $\Delta H_{(T)}$ ,  $\Delta S_{(T)}$ , and  $\Delta G_{(T)}$  thus calculated are plotted as a function of urea concentration at various temperatures. The  $\Delta H_{(T)}$  and  $\Delta S_{(T)}$  change linearly with urea concentration such that the  $\Delta G_{(T)}$  decreases linearly with an increase in urea concentration, as expected from LEM. Yet we would like to bring to notice one feature in our data as represented in Figure 5. Though the  $\Delta H$  and  $\Delta S$  do change with increasing urea concentration, the values

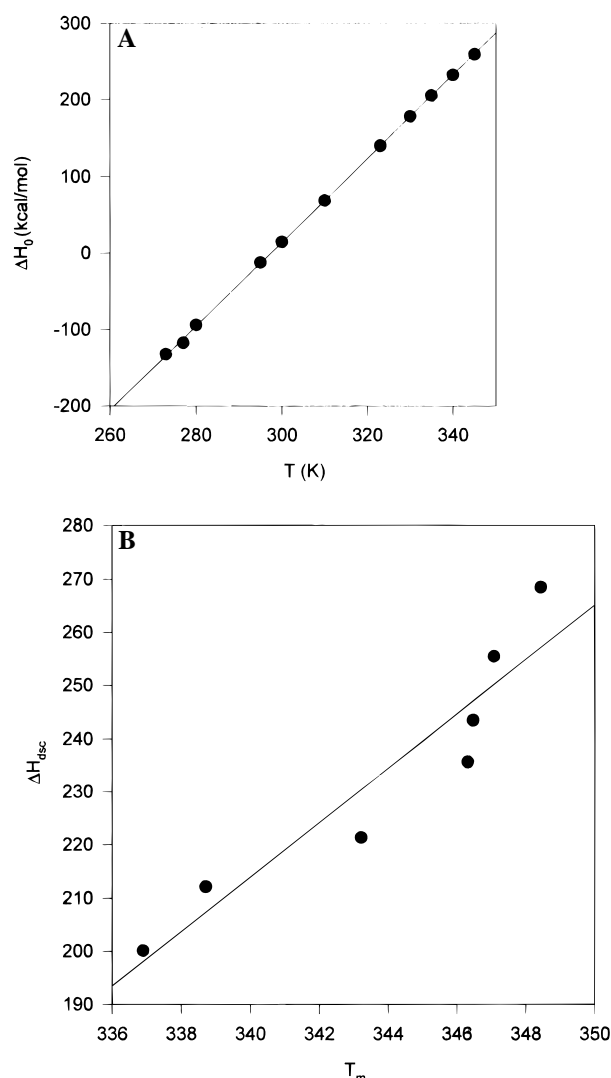


FIGURE 6: (A)  $\Delta H_T$  at 0 M urea (obtained from the y-intercepts of figure 5A) versus the respective temperatures.  $\Delta H_T$  at 0 M urea is obtained from the y-intercepts of figure 5A. The slope of this plot yields the value for  $\Delta C_p$ . (B) Calorimetric enthalpy,  $\Delta H_{\text{dsc}}$  vs  $T_m$ . The slope of this plot yields the value of  $\Delta C_p$ . The differential scanning calorimetric experiments were carried out at various pH's, namely, 4.3, 4.8, 5.2, 5.8, 6.2, 6.8, and 7.2.

of the slopes are different for different temperatures. They seem to increase with higher temperatures. For example, the slopes are  $-4.1$  and  $-0.091$  for  $\Delta H_T$  and  $\Delta S_T$  at 277 K, respectively, and  $1.16$  and  $6.42$  for  $\Delta H_T$  and  $\Delta S_T$ , at 310 K, respectively. This seems to suggest that the urea–pea lectin interactions are effected by temperature.

The  $\Delta C_p$  for unfolding can also be obtained by extrapolating the linear plots of Figure 5A, namely,  $\Delta H_T$  versus urea, to 0 M urea. The values of  $\Delta H_T$  thus obtained (0 M urea) may then be plotted against the respective temperatures (Figure 6A), the slope of which (according to eq 1) should give  $\Delta C_p$ . The value thus obtained was  $5.4$  kcal/(mol K), very close to that obtained when the stability curves (Figure 3A, Table 2) obtained from urea denaturation and thermal denaturation profiles are fitted directly to eq 4. In addition, data from differential scanning calorimetric studies carried at various pHs, are provided in Table 3 and in Figure 6B. The slope for the plot of  $\Delta H_{\text{dsc}}$  vs  $T_m$  gives the value of  $\Delta C_p$  as  $5.12$  kcal/(mol K), very close to that obtained from the above solution denaturation experiments. The heat

Table 3: Data Obtained from the Differential Scanning Calorimetric Studies of Pea Lectin as a Function of pH<sup>a</sup>

| pH  | $T_m$ (K) | $H_{\text{dsc}}$ (kcal/mol) |
|-----|-----------|-----------------------------|
| 4.3 | 336.9     | 200.1                       |
| 4.8 | 338.71    | 212.13                      |
| 5.2 | 343.22    | 221.32                      |
| 5.8 | 346.32    | 235.64                      |
| 6.2 | 346.47    | 243.46                      |
| 6.8 | 347.08    | 255.46                      |
| 7.2 | 348.44    | 268.48                      |

<sup>a</sup> The slope of the plot of  $\Delta H_{\text{dsc}}$  vs  $T_m$  gives  $\Delta C_p = 5.12$  kcal/(mol K).

capacity change,  $\Delta C_p$ , as obtained from the thermal denaturation profiles, shows a very small increase with an increase in urea concentration (Figure 5D). The straight line through the data has a slope of  $0.178$  cal/(mol K M), which represents the change in heat capacity associated with the preferential interaction of urea with the unfolded protein over that of the folded protein. The  $\Delta C_p$  is directly related to changes in the water accessible area upon unfolding (33). Thus the addition of urea into the solution changes the solvent accessibility of polar and nonpolar groups such that a small increase in  $\Delta C_p$  with the increase in denaturant concentration is observed. A similar increase in the  $\Delta C_p$  with the increase in urea concentration has been observed in the case of barstar (24), though no such trend has been observed in the case of  $\beta$ -lactoglobulin (34, 35). Calorimetric studies have indicated that the value of  $\Delta C_p$  for the unfolding of ribonuclease A and lysozyme is higher in the presence of chemical denaturants (36, 37). On the other hand, *Escherichia coli* Hpr protein shows a distinct decrease in  $\Delta C_p$  with increasing urea concentration (25).

In conclusion, the equilibrium unfolding of the dimeric protein, pea lectin, was studied by thermal denaturation and urea-induced unfolding to obtain the thermodynamic parameters as a function of temperature and urea concentrations. Not only does it conform to the simple  $A_2 \rightleftharpoons 2U$  model in its unfolding, but also the data are well-described by the simple linear model for the effects of denaturants on the stability of the protein. The  $A_2 \rightleftharpoons 2U$  transition, in turn, suggests very strong subunit–subunit interactions, perhaps as a consequence of the typical “canonical association”, described above, of the dimers such that dissociation of the dimers to the constituent monomers and their unfolding occur simultaneously. The pea lectin undergoes cold denaturation, which is apparent in the thermal denaturation profiles in the presence of more than  $3.8$  M urea concentration. Moreover, the  $\Delta C_p$  for protein unfolding seems to be quite high at about  $5.3$  kcal/(mol K), a value very close to that obtained from DSC studies (Table 3). A positive change in heat capacity is the hallmark of processes, such as unfolding, that expose nonpolar surfaces to water. The resulting formation of cages of structured water around apolar residues could be the cause of the increase in heat capacity of the solution upon protein unfolding (1). The large heat capacity change for the unfolding of pea lectin may, thus, be a reflection of a larger buried hydrophobic core in the folded protein. This in turn may explain the high conformational stability  $\Delta G_s$ ,  $18.79$  kcal/mol, for the protein, which is much higher than the values for small monomeric proteins and the small Arc dimer (9). The Arc dimer, in addition, has a smaller heat capacity change, perhaps reflecting its small hydrophobic core (11).

On the other hand, fairly large dimers (number of residues per monomer about 100 or more) also have fairly high values of  $\Delta G_u$  (14 kcal/mol and more), a correlation which by no means is exact and proportional (11). For instance the nerve growth factor, has a residue number 118 and  $\Delta G_s = 19.3$  kcal/mol (12), while human glutathione S-transferase, (221 residues) and porcine lung glutathione S-transferase (207 residues) have  $\Delta G_s$  values of 27.8 and 25.3 kcal/mol, respectively (38, 39). The trp aporepressor has 107 amino acids and  $\Delta G_s = 18.2$  kcal/mol (40). It would thus be interesting to possibly, though perhaps empirically, correlate stability (defined by  $\Delta G_s$ ) with the extent of the hydrophobic core (defined by  $\Delta C_p$ ) and the oligomer size (defined by  $M_r$  of the oligomer and the number of residues per monomer). Thus, both Arc repressor (number of amino acids, 53) and Troponin C  $\text{Ca}^{2+}$  binding III peptide (number of residues, 34) have relatively low  $\Delta G_s$  and  $\Delta C_p$ , 9.5 kcal/mol and 1.6 kcal/(mol K) and 11.5 kcal/(mol K), and 0.74 respectively (9, 41). The latter examples, though, caution one that such a correlation, between size, stability, and hydrophobicity, may not be exact and is perhaps empirical. In addition, stabilization may also be a result of disulfide linkages, where such exists. In this context, the present study on the stability of pea lectin assumes significance as both the stability ( $\Delta G_s$ ) and the change in heat capacity are fairly high. Another point, which may be more general to oligomeric proteins, is that a significant percentage of the conformational stability of the oligomer may be contributed by the quaternary interactions alone and that the isolated monomer is stabilized to a much lesser extent, if at all (11).

Thus, pea lectin can now serve as a model for studying the comparative thermodynamics of unfolding of fairly large oligomeric proteins, and also to understand the energetics, the role of quaternary interactions, and the influences of glycosylation on the overall stability and integrity of legume lectins, the "natural mutants of quaternary structures", work which is now in progress for other members of the family.

## ACKNOWLEDGMENT

We thank Dr. Raghavan Varadarajan for critical reading of the manuscript and Alokesh Goshal and C. Ganesh for discussions.

## REFERENCES

1. Tanford, C. (1968) *Adv. Protein Chem.* 23, 121–282.
2. Kim, B. L., and Baldwin, R. L. (1982) *Annu. Rev. Biochem.* 51, 459–489.
3. Privalov, P. L., and Gill, S. J. (1988) *Adv. Protein Chem.* 39, 191–235.
4. Barrick, D., and Baldwin, R. L. (1993) *Protein Sci.* 2, 869–876.
5. Robertson, A. D., and Baldwin, R. L. (1991) *Biochemistry* 30, 9907–9914.
6. Mathews, C. R. (1993) *Annu. Rev. Biochem.* 62, 653–683.
7. Albert, T., and Mathews, B. W. (1987) *Methods Enzymol.* 154, 511–534.
8. Matsumura, M., Becktel, W. J., and Mathews, B. W. (1988) *Nature* 334, 406–410.
9. Bowie, J. U., and Sauer, R. T. (1989) *Biochemistry* 28, 7139–7143.
10. Liang, H., and Terwillinger, T. C. (1991) *Biochemistry* 30, 2772–2782.
11. Neet, K. E., and Timm, D. E. (1994) *Protein Sci.* 3, 2167–2174.
12. Timm, D. E., de Haseth, P. L., and Neet, K. E. (1994) *Biochemistry* 33, 4667–4676.
13. Sharon, N., and Lis, H. (1990) *FASEB J.* 4, 3198–3208.
14. Schwarz, F. P., Puri, K. D., and Surolia, A. (1991) *J. Biol. Chem.* 266, 24344–24350.
15. Surolia, A., Sharon, N., and Schwarz, F. P. (1996) *J. Biol. Chem.* 271, 17697–17703.
16. Schwarz, F. P., Puri, K. D., Bhat, R. G., and Surolia, A. (1993) *J. Biol. Chem.* 268, 7668–7677.
17. Einspahr, H., Parks, E. H., Suguna K., Subramanian, E., and Suddath, F. L. (1986) *J. Biol. Chem.* 261, 16518–16527.
18. Agarwal, B. B. L., and Goldstein, I. J. (1967) *Biochim. Biophys. Acta* 147, 262–271.
19. Bhattacharyya, L., Brewer, C. F., Brown, R. D., and Koenig, S. H. (1985) *Biochemistry* 24, 4974–4980.
20. Pace, N. C. (1990) *Trends Biochem. Sci.* 15, 14–17.
21. Schellman, J. A. (1994) *Biopolymers* 34, 1015–1026.
22. Schellman, J. A. (1978) *Biopolymers* 17, 1305–1322.
23. Schellman, J. A. (1987) *Biopolymers* 26, 549–559.
24. Agashe, V. R., and Udgaonkar, J. B. (1995) *Biochemistry* 34, 3286–3299.
25. Nicholson, E. M., and Scholtz, J. M. (1996) *Biochemistry* 35, 11369–11378.
26. Ganesh, C., Shah, A. N., Swaminathan, C. P., Surolia, A., and Varadarajan, R. (1997) *Biochemistry* 36, 5020–5028.
27. Novokhatny, V., and Ingham, K. (1997) *Protein Sci.* 6, 141–146.
28. Arunachalam, V., and Kellis, J. T. (1996) *Biochemistry* 35, 11379–11385.
29. Greene, R. F., and Pace, N. C. (1974) *J. Biol. Chem.* 249, 5388–5393.
30. Schellman, J. A. (1990) *Biophys. Chem.* 37, 121–140.
31. Schellman, J. A., and Grassner, N. C. (1996) *Biophys. Chem.* 59, 259–275.
32. Tanford, C. (1970) *Adv. Protein Chem.* 21, 1–95.
33. Murphy, K. P., and Freire, E. (1992) *Adv. Protein Chem.* 43, 313–361.
34. Pace, N. C., and Tanford, C. (1968) *Biochemistry* 7, 198–208.
35. Girko, Y. V., and Privalov, P. L. (1992) *Biochemistry* 31, 8810–8815.
36. Pfeil, W., and Privalov, P. L. (1976) *Biophys. Chem.* 44, 33–40.
37. Makhataze, G. I., and Privalov, P. L. (1992) *J. Mol. Biol.* 226, 491–505.
38. Wallace, L. A., and Sluis-Cremer, N. (1998) *Biochemistry* 37, 5320–5328.
39. Dirr, H. W., and Reinemer, P. (1991) *Biochem. Biophys. Res. Commun.* 180, 294–300.
40. Gittelman, M. S., and Matthews, C. R. (1990) *Biochemistry* 29, 7011–7020.
41. Monera O. D., Shaw, G. S., Zhu, B. Y., Sykes, B. D., Kay, C. M., and Hodges, R. S. (1992) *Protein Sci.* 1, 945–955.

BI9811720